We have shown above that a formula of the form (10) or even (11), with properly chosen parameters, can be made to fit experimental data over a wide range with a high accuracy. Similar results[1,2] were previously obtained for the light elements with an even more detailed expression which exhibited the dependence of binding energies on isotopic spin.

Although these expressions were derived for the shell model, their simplicity does not allow one to believe that they are peculiar to the shell model alone. Also, the fact that only relatively small changes in the parameters occur as long as one remains within a major shell, may indicate that the expression obtained is a result of the observed grouping of nucleons into shells, rather than being due to the detailed structure of the shell model. To investigate this point further, it is necessary to see to what extent can the parameters be derived from the shell-model wave functions and a given two-body interaction. Further work along these lines is being done here.

PHYSICAL REVIEW VOLUME 108, NUMBER 2 OCTOBER 15, 1957

π^--p Elastic Scattering at 1.44 Bev*

M. CHRETIEN†, J. LEITNER‡, N. P. SAMIOS, M. SCHWARTZ,§ AND J. STEINBERGER
Nevis Cyclotron Laboratories, Physics Department, Columbia University, Irvington-on-Hudson, New York
(Received June 17, 1957)

An investigation of π^-+p elastic scattering, made in a liquid propane bubble chamber, is reported. Identification of events is made on the basis of kinematics. The problem of contamination by pion scattering from protons bound in carbon is considered in some detail; it is shown that the latter requires a correction of only $4\pm2.5\%$ of the total number of events. The angular distribution is presented. It shows a large diffraction peak at small angles and an approximately isotropic plateau over the backward hemisphere. The forward peak is fitted to a black-sphere diffraction pattern with a radius of $(1.08\pm0.06)\times10^{-13}$ cm. The total elastic cross section is found to be $\sigma_e=10.1\pm0.80$ mb.

INTRODUCTION

We report here some results of the elastic scattering of 1.3-Bev (kinetic energy) negative pions obtained in an exposure of a propane bubble chamber, previously analyzed to study strange particle production.[1]

The study of πp scattering in the Bev range has been in progress for some years now, using the hydrogen diffusion cloud chamber.[2–4] Our results are not qualitatively different, but are more extensive. From an experimental point of view, perhaps of greatest interest is the demonstration made in some detail in this paper, that the elastic hydrogen events may be differentiated quite clearly from other events found in the chamber. The pion beam is collimated, shielded, and magnetically analyzed as shown in Fig. 1. The resulting spread in beam energy deduced from trajectories plotted through the collimation system,[5] is $\pm1\%$. The absolute value of the pion beam momentum is 1.433 ± 0.015 Bev/c. This is determined, as explained in (1), from a study of two unstable-particle production events which were obtained in the same exposure.

The liquid propane bubble chamber has previously been described[6,7]; it is $6\frac{1}{8}$ in. in diameter and 4 in. in depth. The density of expanded propane is 0.429 g/cm^3; the partial density of hydrogen is 0.078 g/cm^3. There is no magnetic field.

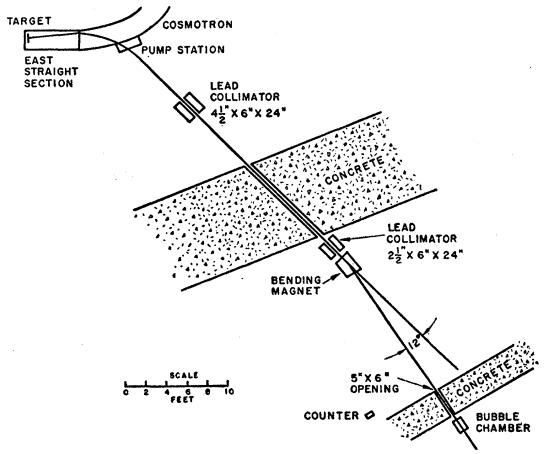

FIG. 1. Experimental setup showing π-beam trajectory collimators, bending magnet, and position of chamber.

* This research was supported by the Atomic Energy Commission and the Office of Naval Research.
† Now at Brandeis University, Boston, Massachusetts.
‡ Now at Duke University, Durham, North Carolina.
§ Now at Brookhaven National Laboratory, Upton, Long Island, New York.
[1] Budde, Chretien, Leitner, Samios, Schwartz, and Steinberger, Phys. Rev. **103**, 1827 (1956).
[2] Eisberg, Fowler, Lea, Shephard, Shutt, Thorndike, and Whittemore, Phys. Rev. **97**, 797 (1955).
[3] W. D. Walker and J. Crussard, Phys. Rev. **98**, 1416 (1955).
[4] W. D. Walker (to be published).
[5] We would like to thank R. Sternheimer for calculating these trajectories for us.
[6] Leitner, Samios, Schwartz, and Steinberger, Nevis Cyclotron Report No. R-105, Nevis No. 10 (unpublished).
[7] J. Leitner, Nevis Cyclotron Report No. R-140, Nevis No. 28 (unpublished).

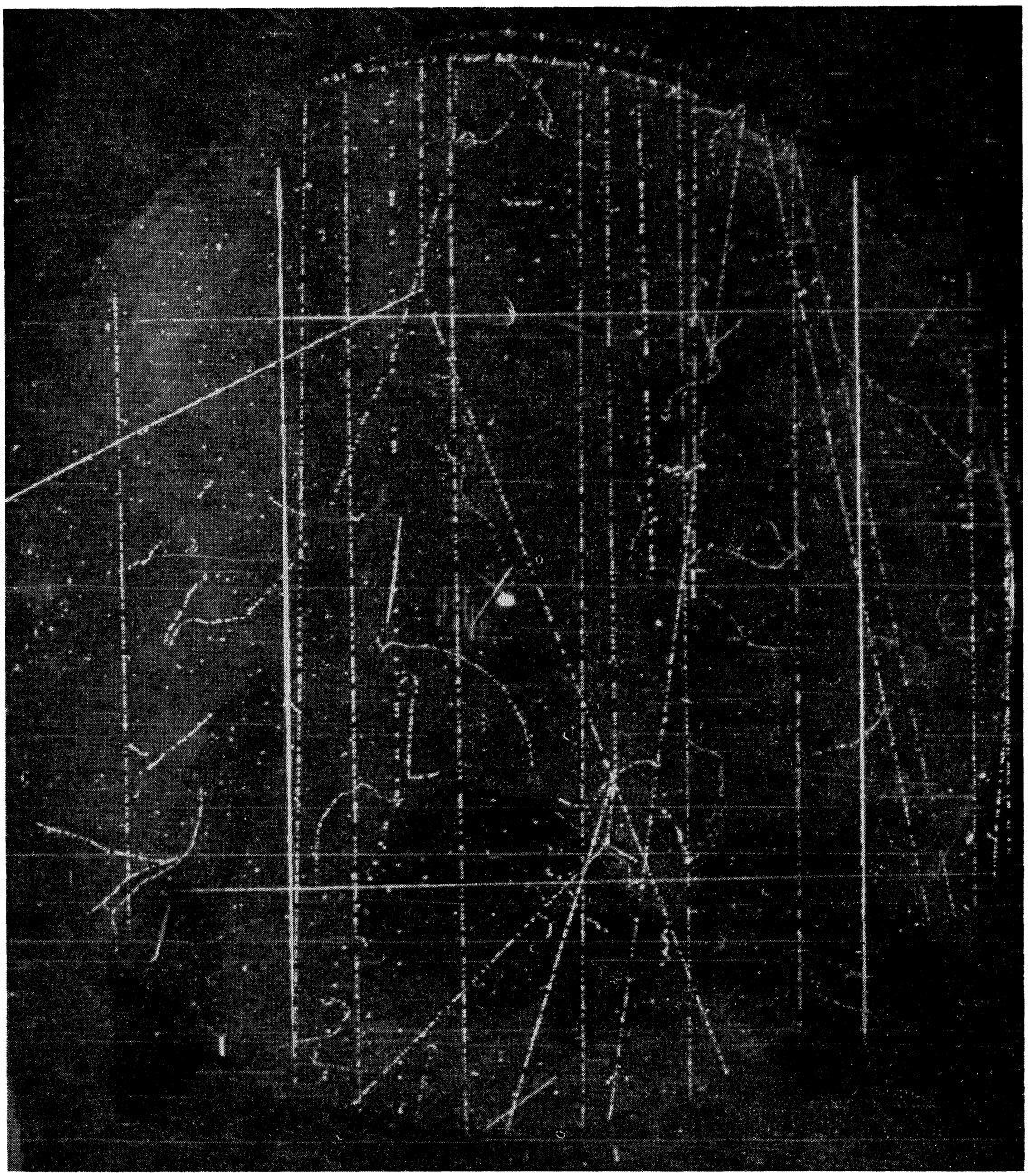

FIG. 2. Bubble chamber photograph of a typical elastic scattering event.

Altogether, 14 300 stereoscopic pictures were taken with an average of 14 tracks per picture. The pictures are examined for two-prong stars produced by beam tracks. Scanning is done by looking along each track for interactions. All pictures are rough-scanned twice. After the events are located, the coordinates of the vertex and the angles between the tracks in both stereo views are measured with an accuracy of the order of $\pm 0.3°$. The space angles, and other quantities necessary for the analysis of the event, are then computed electronically. A typical π^--p elastic scattering event is shown in Fig. 2.

II. SELECTION OF THE EVENTS

A two-prong star, in order to be classified as an elastic hydrogen event, must satisfy the following criteria within the limits of error of the measurements.

1. It must be coplanar. As a measure of coplanarity we employ the triple scalar product (C) of the three unit vectors defined by the two-prong star. The pre-

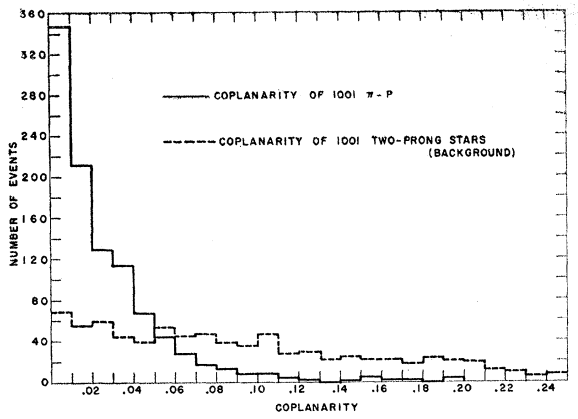

FIG. 3. Values of the triple scalar product, C, for 1001 πp events (solid line) and 1001 two-prong stars (background).

cision of this measurement depends not only on the lengths of the tracks, but also on the orientation of the plane of event. The dependence of C upon these effects is discussed in detail in reference 7. Figure 3 shows the values of the triple scalar product (C) of all those events accepted as "coplanar," as well as a representative sample of rejected events.

2. The angular correlation of the recoil proton and scattered pion must be consistent with the kinematics for the process. We show in Fig. 4, the kinematic curve in the laboratory system for 1.44-Bev (total energy) pions, together with two curves which show the probable error of measurement, along with those events which have been accepted as elastic π-p's. The probable error in the space angle is shown as $\pm 1.5°$; this results from a $\pm 0.3°$ average error in the projected-angle measurement. Approximately 92% of the accepted events lie within the acceptance region shown in Fig. 4.

3. The ranges of any stoppings in the liquid must be consistent with those expected from the π-p kinematics. This criterion, the most sensitive of the four, is applied to an appreciable number of the cases (30%) since the diffraction scatterings show a short low-energy proton recoil. [A proton track of 3 in. in our chamber corresponds to a proton energy of 68 Mev and a pion scattering angle of 30° in the center-of-mass (c.m.) system.]

4. The bubble densities and multiple scatterings of the tracks must be consistent with those expected from the known energies and momenta. This criterion is applied qualitatively.

In all, ~3000 stars were measured, calculated, and analyzed. Of these, 1027 were selected as satisfying the above criteria.

III. CONTRIBUTION OF THE CARBON EVENTS

The selection criteria are such that all events consistent with being elastic hydrogen events are accepted, provided only that they are detected. All detected hydrogen events are therefore presumably accepted, but in addition we accept some carbon events which accidentally happen to satisfy the criteria. Below we make an attempt to estimate the number of such events from protons bound in carbon, and this number will be subtracted from the total number of events.

To this end, we have plotted in Fig. 5, the angular correlation of those 562 events which *are coplanar but do not satisfy one or more of the remaining acceptance criteria*. For the sake of definiteness, the smaller of the two scattering angles is plotted against the larger. On the same figure we have also plotted four lines which delineate three areas: A central region B which corresponds to the region in which 92% of the accepted events were found, and the adjacent regions A and C drawn so that the combined area of A and C is equal to that of B.

Firstly, we point out that it is clear from Fig. 5 that the background events are not particularly peaked in

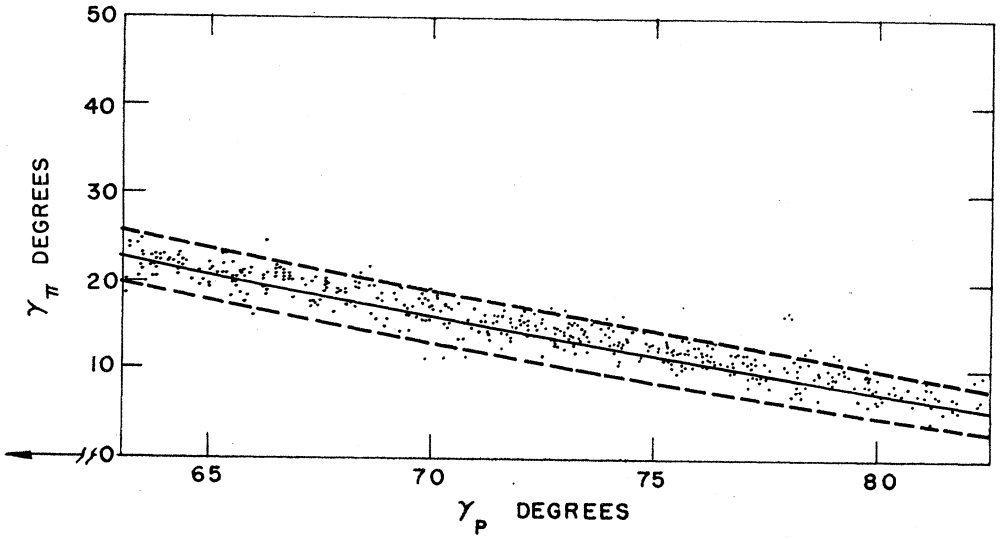

FIG. 4. A portion of the angular correlation plot of elastic π-p events. The solid line is the kinematic curve for incoming pions of 1.44 Bev (total energy). The dotted envelope covers the region of probable error, $\pm 1.5°$ wide.

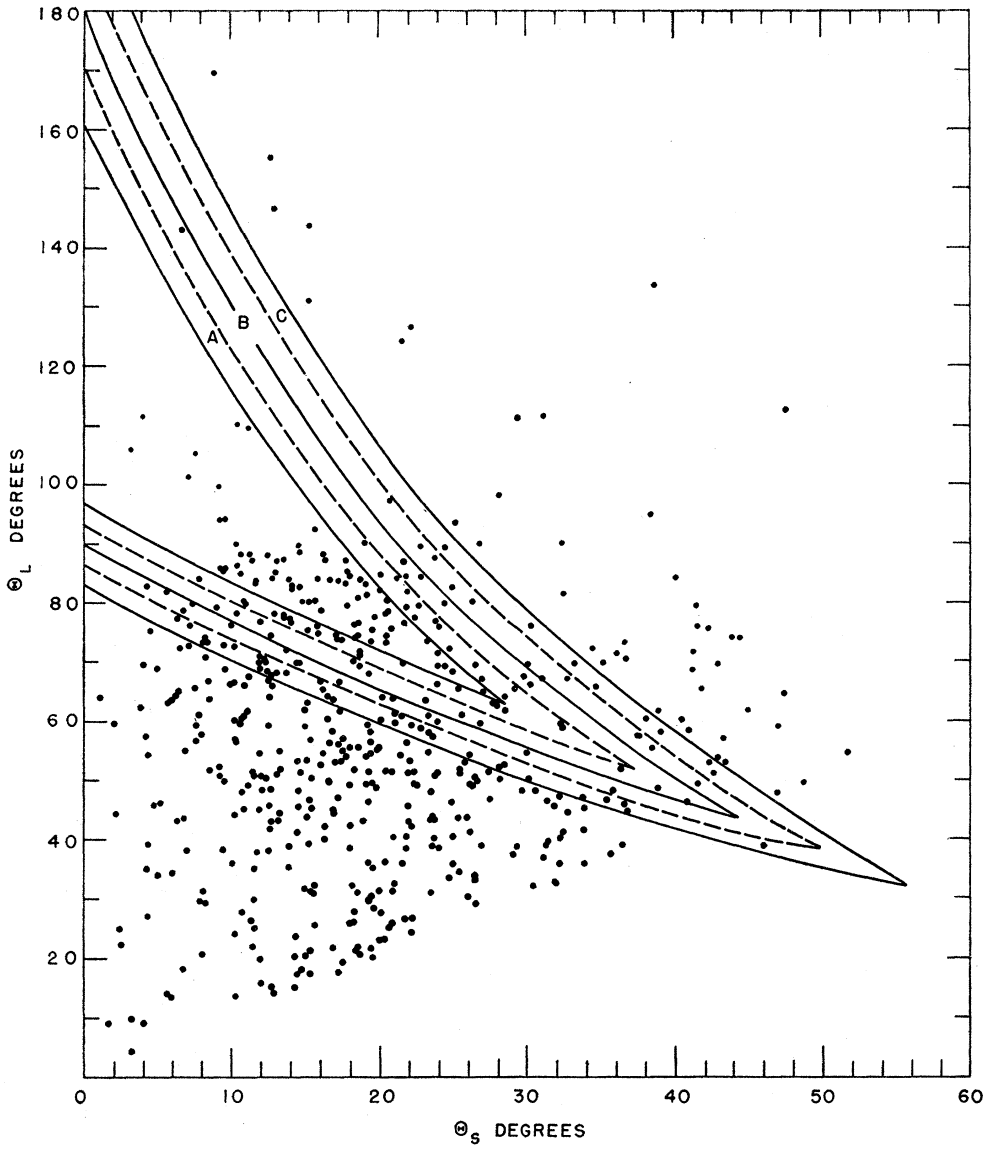

FIG. 5. Angular correlation of coplanar ($C \leq 0.06$) two-prong star background events. Dashed lines correspond to acceptance region B (see Fig. 4). Solid lines encompass an additional region (A+C) whose area is equal to that of B.

the vicinity of the π-p scattering curve. The carbon background which is included in our results can therefore be estimated by subtracting the carbon events in the acceptance region (B) from those in the adjacent region (A+C). This is not completely well defined because the acceptance region is not well defined. The allowed deviation in the kinematics of any particular event depends on the measureability of that event. We have arbitrarily taken a region which contains a rather large fraction (92%) of the events. In this way we believe the error is overestimated. The number of erroneously included carbon events is then probably somewhat smaller than

$$105-66=39\pm\{[(105)^2+(66)^2]^{\frac{1}{2}}\}=39\pm12,$$

and the percentage correction is $39/1029=(4\pm2.5)\%$. The indicated error is taken larger than the statistical error to include the uncertainty in the width of the acceptance strip. It is clear that the error due to the inclusion of carbon events will be small.

IV. FIDUCIAL REGION AND SCANNING EFFICIENCY

The spatial positions of the vertices of 1027 accepted events were measured. The distribution in depth is shown in Fig. 6 and the distribution in the plane of the chamber is shown in Fig. 7. We chose, for the fiducial region, a right circular cylinder 7.5 cm in depth and 12 cm in diameter. The axis of this cylinder is parallel to the axis of the chamber, but displaced $\frac{1}{2}$ cm

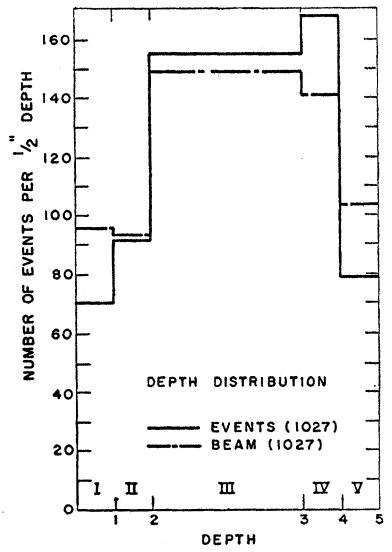

FIG. 6. Depth distribution of 1027 elastic πp events (solid line), and 1027 beam tracks (dashed line).

(in the direction of beam) from the geometric center of the chamber; see Fig. 7. Within this region the detection probability seems uniform. Eight hundred fifty of the 1027 accepted events are within the fiducial region; *all results will be based on these 850 events.*

Even within this region, however, we do not find all events. The detection efficiency depends upon both the scattering angle and the dip angle. Events with a large dip angle are harder to recognize and so are those in which the proton recoil is very short, i.e., the scattering angle is too small. For center-of-mass scattering angles greater than 15°, however, the detection efficiency should be near unity for events whose planes are reasonably parallel to the chamber plane.

In Fig. 8, we have plotted the number of events within a certain range of the (pion) scattering angle as a function of the azimuthal angle. This gives the following estimates for the ratio of the detection efficiency to its

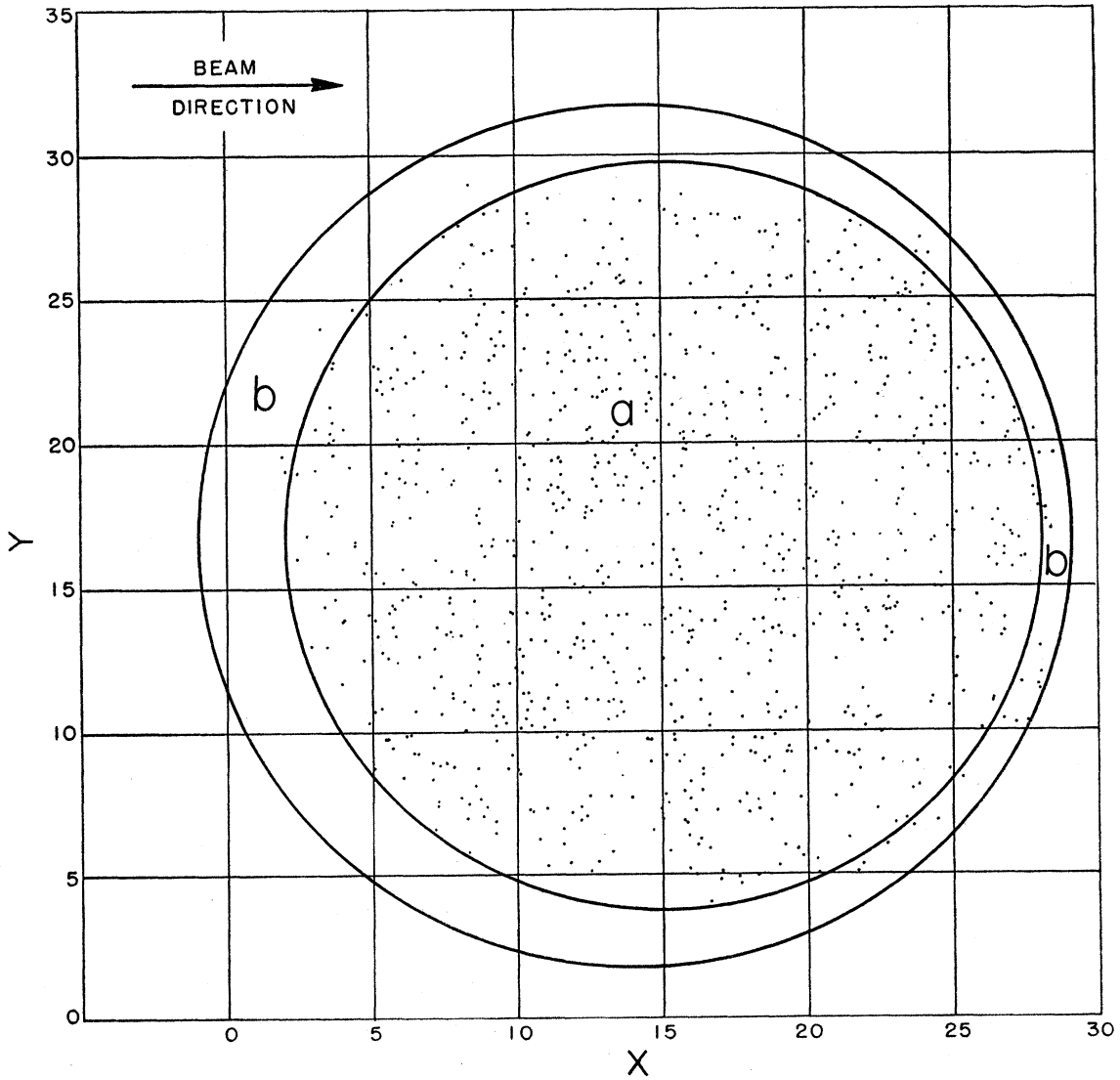

FIG. 7. Plot of the vertices of 1027 elastic πp events in the chamber plane. The arrow indicating beam direction should be reversed.

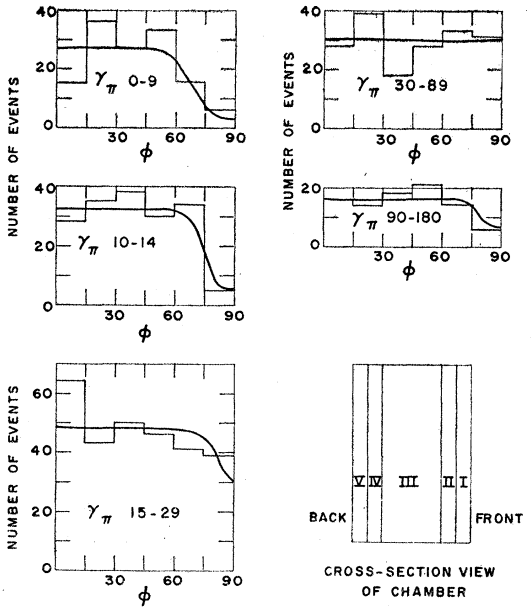

FIG. 8. Plots of the number of observed events *vs* the azimuthal angle as a function of the laboratory scattering angle γ, for the accepted πp elastic events, found in the fiducial region.

value for small azimuthal angles:

Center-of-mass scattering angle:	10°–15°	15°–30°	30°–150°	150°–180°
Efficiency:	0.86	0.97	1.00	0.925

For the small azimuthal angles the absolute efficiency was found by comparison of several independent scannings, to be 0.93 ± 0.04.

V. RESULTS

The cross section is proportional to the number of events divided by the total track length. The track length is determined by measuring in every 50th picture the projected track length within the fiducial region and multiplying by 50. The total pion path length found in this way is $L=2.25\times10^6$ cm$\pm2\%$. It is necessary to subtract the muon and electron track lengths from L. The muon contamination is estimated to be $(4\pm3)\%$ from the work of Cool, *et al.*[8] For the estimation of the electron background we rely on the experiments of Lindenbaum and Yuan.[9] According to their results, the electron contamination can be neglected at this energy. The corrected total track length is 2.16×10^6 cm.

A histogram of the 850 observed events is given in Fig. 9 as a function of the center-of-mass scattering angle and this is converted to the differential cross section of Fig. 10, using the track length discussed above, the scanning efficiencies discussed in V, the correction for carbon contamination discussed in III, and the density of expanded propane at 60°C ($\rho=0.429$ g/cm^3).

The cross section at 0° cannot be determined here as discussed above; however, it can be determined quite independently from the measurement of the total cross sections and the elastic π^--p and π^+-p cross sections at all energies, with the help of the dispersion relations. From the total cross section of 30 ± 3 mb[10] at this energy, we get for the imaginary part of the forward coherent scattering amplitude: $\mathrm{Im}f_c(0)=\sigma_T/4\pi\lambda$ $=(0.853\pm0.09)\times10^{-13}$ cm. From the dispersion relations,[11] Sternheimer[12] gets for the real part of the forward coherent scattering amplitude:

$$\mathrm{Re}f_c(0)=-0.3\times10^{-13}\text{ cm}.$$

Thus,

$$(d\sigma/d\Omega)_{\text{coherent}}(0°)=8.2\pm1.6\text{ mb}.$$

At 0° the spin-flip cross section vanishes, and hence the forward coherent cross section is equal to the forward elastic cross section. The latter point at 0° has also been plotted in the results shown in Fig. 10.

The total elastic cross section can be obtained by integrating the curve of Fig. 10. This gives $\sigma_{\text{el}}(\pi^-p)$ $=10.1\pm0.8$ mb. The major contribution (0.6 mb) to the total error arises from the uncertainties in the scanning efficiency correction.[13]

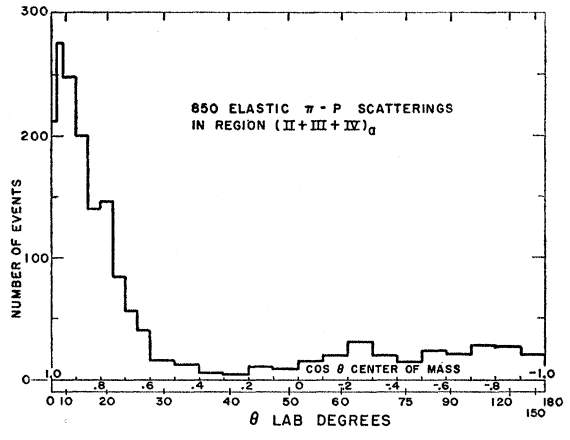

FIG. 9. Uncorrected angular distribution of the 850 elastic πp scatterings in the fiducial region.

VI. DISCUSSION OF RESULTS

The angular distribution of Fig. 10 is peaked in the forward direction, falls to a low value (perhaps close to 0) near 60° (c.m.), and then rises to a rather uniform level of ~0.3 mb between 90° and 180° (c.m.). The forward contribution is most certainly the diffraction

[8] Cool, Piccioni, and Clark, Phys. Rev. **103**, 1082 (1956).
[9] S. Lindenbaum (private communication).
[10] Cool, Madansky, and Piccioni, Phys. Rev. **94**, 736 (1954).
[11] Goldberger, Miyazawa, and Oehme, Phys. Rev. **99**, 986 (1955).
[12] R. Sternheimer, Phys. Rev. **101**, 384 (1956).
[13] This is true, if one assumes that the dispersion relations hold at the energy under consideration. There is some evidence, in fact, that deviations from the $\mathrm{Re}f_c(0°)$ predicted by the dispersion relations exist even at lower energies. [See G. Puppi and A. Stanghellini, Nuovo cimento **5**, 1305 (1957).] If the dispersion relations do not hold here, a complete re-estimation of σ_{el} will be required.

scattering which is a consequence of the large absorption; ($\sigma_{abs} \sim 20$ mb, $\sigma_{total} \sim 30$ mb). However, the backward scattering is much too large to be attributed to the same cause. The analysis is further complicated by the fact that the model for discussing the forward peak and the backward plateau must probably be different, but their amplitudes interfere; it is probably not, therefore, possible to discuss the diffraction peak and the observed minimum without taking this interference into account.

At this time we wish to extract from the data only the effective pion-nucleon interaction radius. Even this is made slightly dubious by the interference of the diffraction and nondiffraction scattering amplitudes, the latter being entirely unknown. We therefore fit the theoretical diffraction amplitude to two points, both at small angles (15° and 30° c.m.), where the diffraction amplitude most probably strongly dominates the nondiffraction amplitude. The radius of the rectangular well, R, must be $(1.08 \pm 0.06) \times 10^{-13}$ cm in order that the observed points fit a diffraction pattern $|J_1(kr \sin\theta)/kr \sin\theta|^2$, where k is 3.58×10^{13} cm^{-1}. This curve is shown in Fig. 10 as the solid line. We emphasize that no fit is expected except for the main part of the forward peak.

The above value for R is considerably larger than the value deduced by Hofstadter *et al.*[14] from the electron-proton scattering at 550 Mev, where a good fit is obtained by taking a Gaussian extension for the proton of rms radius 0.8×10^{-13} cm. This smaller effective radius must result in a considerably broader pattern and cannot fit our results. This need not surprise one, since *a priori*, there is no clear connection between the electrostatic interaction and the meson-nucleon interaction.

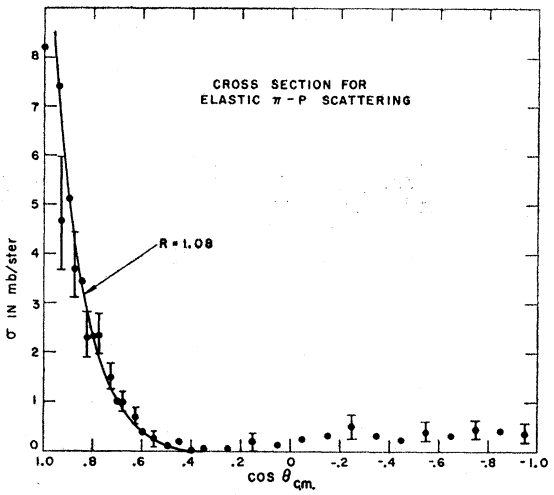

FIG. 10. Corrected differential cross section. The point at 0° is not measured; it is found from the total cross section and the $\pi^- p$, $\pi^+ p$ cross sections at all energies as described in VI. The solid curve is a black-sphere diffraction pattern for $R = 1.08 \times 10^{-13}$ cm. Some representative statistical errors are shown.

[14] R. Hofstadter *et al.*, *Proceedings of the Sixth Annual Rochester Conference on High-Energy Physics*, 1956 (Interscience Publishers, Inc., New York, 1956), Sec. 9.

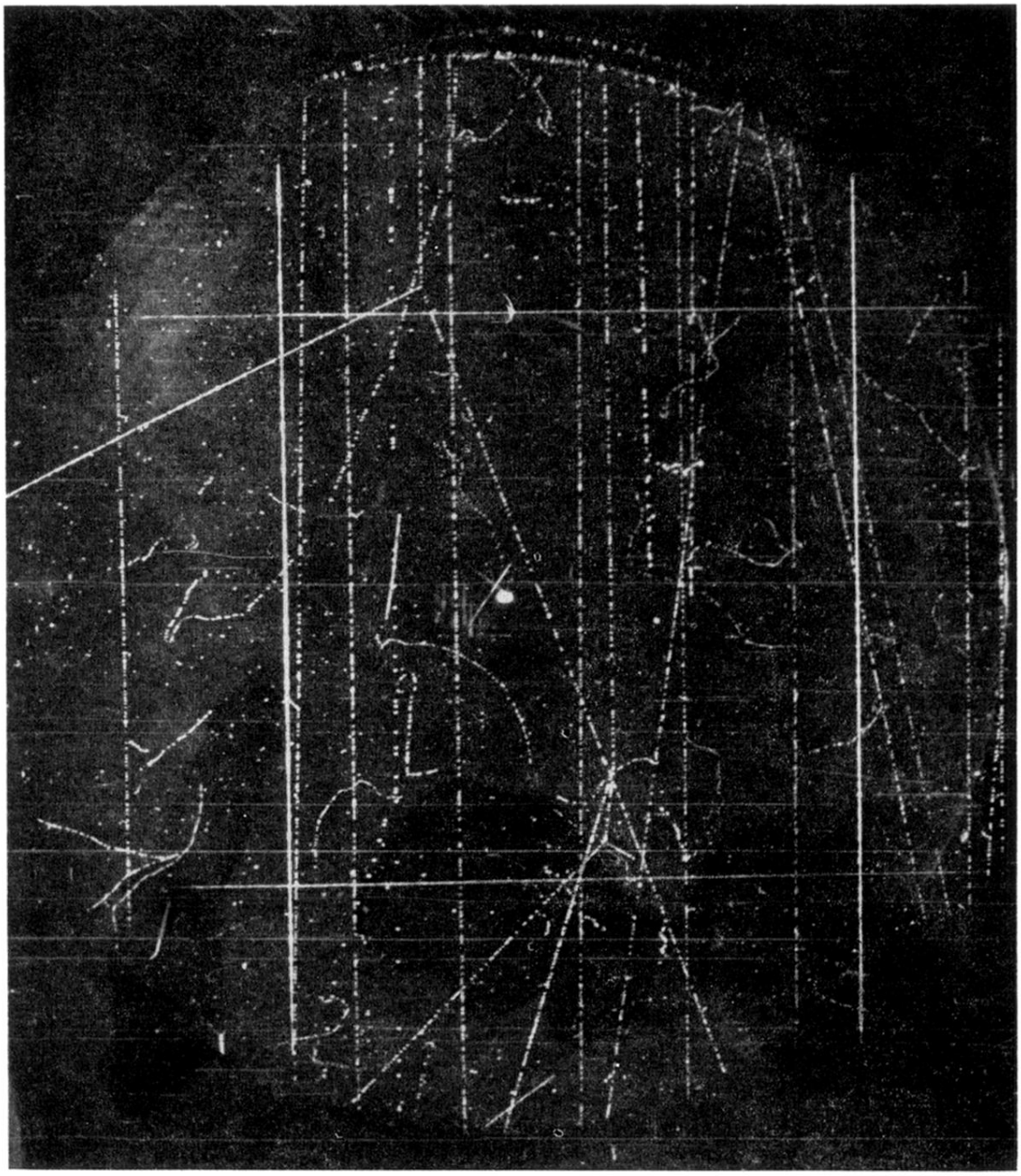

FIG. 2. Bubble chamber photograph of a typical elastic scattering event.